33rd Annual International Conference of the IEEE EMBS
Boston, Massachusetts USA, August 30 - September 3, 2011

A Concurrent Comparison of Inertia Sensor-Based Walking Speed Estimation Methods

Annemarie Laudanski, Shuozhi Yang, and Qingguo Li

Abstract **This study performed a concurrent comparison of two walking speed estimation methods using shank- and foot-mounted inertial measurement units (IMUs). Based on the cyclic gait pattern of the stance leg during walking, data was segmented into a series of individual stride cycles. The angular velocity and linear accelerations of the shank and foot over each of these cycles were then integrated to determine the walking speed. The evaluation was performed on 10 healthy subjects during treadmill walking where known treadmill speeds were compared with the estimated walking speeds under normal and toe-out walking conditions. Results from the shank-mounted IMU sensor yielded more accurate walking speed estimates, with a maximum root mean square estimation error (RMSE) of 0.09 m/s in normal walking and 0.10 m/s in toe-out conditions; while the foot-mounted IMU sensors yielded a maximum RMSE of 0.14 m/s in normal walking and 0.26 m/s in toe-out conditions. Shank-mounted IMU sensors may prove to be of great benefit in accurately estimating walking speeds in patients whose gait is characterized by abnormal foot motions.**

I. Introduction

Quantitative gait analysis through portable inertial sensors is becoming a useful tool for clinical assessment of abnormal gait patterns, and objective evaluation of treatment of patients with walking disabilities [1-4]. To acquire spatial-temporal gait information, inertial measurement units (IMU), a combination of accelerometers and gyroscopes, has been used for estimating walking speeds [5-7]. Previous studies took advantage of the cyclic nature of walking as well as the key gait events, such as foot flat and shank vertical, in each stride to estimate the corresponding walking speeds and correct the bias errors in the acceleration measurements. With the measurements from the IMU sensor attached to different body locations, one class of the walking speed estimation methods directly integrates the sensor accelerations in the global coordinate system to determine the sensor displacement and thus, the stride-by-stride walking speed. The local-to-global frame acceleration coordinate transformation is achieved through continuously monitoring the sensor orientation by integrating angular velocity measured by a gyroscope. For example, Sabatini *et al.* used an IMU sensor mounted to the instep of the foot. During treadmill walking experiments, the proposed direct integration method using foot-mounted sensor achieved accurate estimate on walking speeds with a root mean squared error (RMSE) of 5% [5]. Li *et al.* proposed an alternative approach and attached an IMU sensor to the lateral-aspect of the shank during treadmill walking experiments and reported a RMSE for speed estimation of 7% [6]. Although they both reported a relative small RMSE error, it is impossible to compare the results directly because of the difference in the experimental protocols including speeds and slopes used in the experiments. In addition, both methods were tested with healthy subjects under normal walking conditions, the performance of these two methods under pathological gait conditions require further evaluation before clinical applications.

The purpose of this study was to perform a concurrent performance comparison of the shank- and foot-mounted IMU sensor-based walking speed estimation methods under normal condition and toe-out condition, a condition simulating the pathological gait. We hypothesizes that the foot-mounted sensor and shank-mounted sensor will produce similar results under the normal walking condition, and the performance of the foot-mounted sensor will degrade more than that of the shank-mounted sensor under the toe-out walking condition.

II. Method

A. Experimental Instrumentation

The IMUs used in this study were composed of one tri-axial accelerometer and one tri-axial rate gyroscope (Xsens Technology B.V., Netherlands) [8]. Calibration of the sensors and data collection was conducted using the MVN Studio Pro (Xsens Technologies B.V., Netherlands). All experiments were conducted using a treadmill at 0^o incline (Nordic-Track, Inc., Logan, UT, USA). The data were processed offline and the speed estimation algorithms were programmed using MATLAB (The MathWorks, Natick, MA, USA).

B. Speed Estimation Method

The tri-axial IMUs provide 3-axial acceleration and 3-axial angular velocity measurements. However, our analysis is only concerned about the sagittal plane of motion (plane of progression). Therefore, we only utilize accelerations and angular velocity in the sagittal plane for analysis. In order to perform the concurrent comparison between shank and foot-mounted sensors in estimating walking speed, raw data from both IMUs were collected simultaneously at 120 Hz. A second-order forward-backward low-pass Butterworth filters were applied to raw IMU data, with a cutoff

Manuscript received March 26, 2011. This work was supported in part by NSERC Discovery Grant to Q. Li

A. Laudanski, S. Yang and Q. Li are with the Department of Mechanical and Materials Engineering, Queen's University, Kingston, ON, Canada (phone: 613-533-3191; fax: 613-533-6489; e-mails: a.laudanski@queensu.ca, yangs@me.queensu.ca, qli@me.queensu.ca).

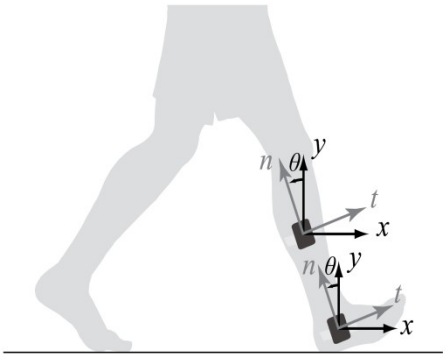

Figure 1 Inertial Measurement Units were attached to the lateral-aspect of each subject's shank and foot. The normal and tangential accelerations were measured along the *n* and *t* axes, respectively. The gyroscope axes lay orthogonally to the plane defined by these axes. The world coordinates were defined as *xoy*, with the vertical axis *y* parallel to gravity. Segment angle, θ, were defined as the angle between the normal accelerometer axes and the vertical world coordinate system axes. As per the right hand rule, positive angular velocities correspond to counter clockwise rotations. Arrows indicate the positive directions of each axis.

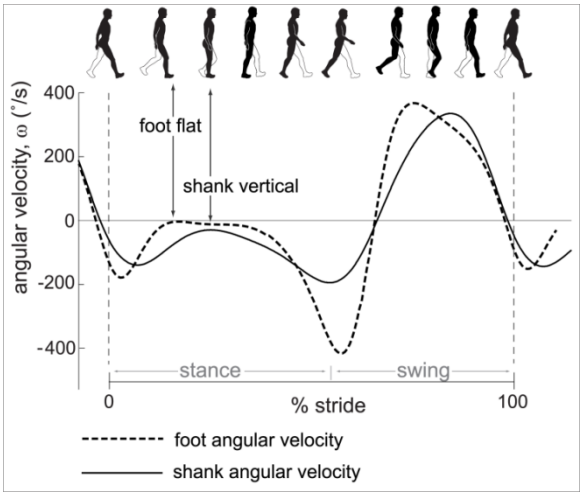

Figure 2 Characteristics of angular velocity,ω, during one stride cycle. At the mid-stance shank vertical event and the foot flat event, the magnitude of the angular velocity of each segment reaches a local minimum with values nearing zero. In symmetry, both segments on the left leg have the same angular velocity characteristics as those on the right leg.

frequency of 2.3 Hz for the shank and 2 Hz for the foot sensor signals. Then, the direct integration-based walking speed estimation algorithms were implemented for each sensor with the filtered data [5-6]. Despite the differences of sensor location, the algorithms for these two sensors share the same structure with three common components as: gait cycle segmentation, acceleration transformation, double integration of the transformed accelerations and acceleration bias correction. The only difference between these two algorithms is the way of determining the initial velocities for the double integration of the transformed accelerations.

As the first step, the continuous walking motion is segmented into a series of stride cycles before the displacements can be computed. For shank-mounted sensor, it was determined by the time in the stance phase when the shank is parallel to the direction of gravity. An inverted pendulum model of the stance leg during walking was used to detect a characteristic features in the shank gyroscope signal (Fig. 2) and determine the shank vertical event [5]. Similarly, the foot sensor signals were also segmented by using the gyroscope signal to detect the foot flat position of each cycle.

To compute the displacements along the horizontal and vertical world coordinate axes, the measured raw acceleration measurements, $a_n(t)$ and $a_t(t)$, at time t are converted into component accelerations $a_x(t)$ and $a_y(t)$ in the world coordinate system according to

$$\begin{bmatrix} a_x(t) \\ a_y(t) \end{bmatrix} = \begin{bmatrix} \cos\theta(t) & -\sin\theta(t) \\ \sin\theta(t) & \cos\theta(t) \end{bmatrix} \begin{bmatrix} a_t(t) \\ a_n(t) \end{bmatrix} - \begin{bmatrix} 0 \\ g \end{bmatrix}, \quad (1)$$

where g is the acceleration due to gravity and $\theta(t)$ is the sensor orientation, computed by integrating the measured angular velocity $\omega(t)$,

$$\theta(t) = \int_0^t \omega(\tau)d\tau + \theta(0), \quad (2)$$

where $\theta(0) = 0$ is the initial segment angle prior to integration. This is an assumption based on that the sensors are aligned perfectly with respect to the limb segments.

The integration of the horizontal and vertical accelerations yield the associated instantaneous horizontal and vertical velocities, $\boldsymbol{v_x(t)}$ and $\boldsymbol{v_y(t)}$,

$$v_x(t) = \int_0^t a_x(\tau)d\tau + v_x(0),$$
$$v_y(t) = \int_0^t a_y(\tau)d\tau + v_y(0), \quad (3)$$

where $v_x(0)$ and $v_y(0)$ are the initial horizontal and vertical velocities, respectively.

The initial velocities for the foot during foot-flat are approximated as 0 m/s for both $v_x(0)$ and $v_y(0)$. However, for the shank, the velocity cycle starts from mid-stance shank vertical event where the angular velocity is not completely zero (Fig. 2). The initial velocity required for integration of (3) could be calculated based on the sensor position and shank angular velocity, assuming the shank is approximately rotating about the ankle joint in the stance phase,

$$v_t(0) = \omega(0) \cdot L, \quad (4)$$

$$\begin{bmatrix} v_x(0) \\ v_y(0) \end{bmatrix} = \begin{bmatrix} \cos\theta(0) \\ -\sin\theta(0) \end{bmatrix} \cdot v_t(0), \quad (5)$$

where $v_t(0)$ is the local shank tangential velocity at the beginning of the stride cycle and $v_x(0)$ and $v_y(0)$ are the horizontal and vertical velocities at the same time, respectively. L is the distance between the shank IMU sensor and the ankle joint. The same method was used to calculate the end stride cycle velocities, $v_{x\text{-}calculated}(T)$ and $v_{y\text{-}calculated}(T)$.

As the acceleration measured by low-cost accelerometers subject to a bias, integration of the biased acceleration over a

small time period will result in velocity drifts. To correct velocity drift, we calculated the difference between the actual velocities measured by gyroscope (Eq. 4 and 5) and the calculated sensor velocity (Eq. 3) at the end of each stride cycle. The corrected sensor velocity can thus be calculated by adding the linear trend difference between actual and calculated sensor velocities to the velocities estimated with integrating accelerations (Eq. 3).

$$v_{x-corrected}(t) = v_x(t) + \frac{v_{x-calculated}(T) - v_x(T)}{T} \cdot t,$$
$$v_{y-corrected}(t) = v_y(t) + \frac{v_{y-calculated}(T) - v_y(T)}{T} \cdot t, \qquad (6)$$

where $v_x(T)$ and $v_y(T)$ are the end stride cycle velocities calculated by integrating the acceleration signals in (3). $v_{x-corrected}(t)$ and $v_{y-corrected}(t)$ are the corrected instantaneous horizontal and vertical velocities based on the end stride cycle angular velocity measurements, respectively.

The corrected instantaneous velocities, $v_{x-corrected}(t)$ and $v_{y-corrected}(t)$, are then integrated to yield the associated instantaneous displacements, $d_x(t)$and $d_y(t)$per stride cycle. Finally, the root sum squared of these displacement values is divided by the time span of each individual stride cycle to obtain the stride-by-stride walking speed. The summation of both components helps to eliminate some of the errors associated with initial sensor misalignment ($\theta(0) \neq 0$).

C. Experimental Method

Five male and five female subjects (height: 1.73 ±0.29 meters; weight: 68.9 ±12.4 kg) participated in the treadmill walking experiments. Before the experiments began, volunteers gave their informed consent to participate in the study in accordance with university policy. We collected data at treadmill speeds of 0.8, 1.0, 1.2, 1.4, and 1.6 m/s over 60s trials for each speed, while the subject wore IMU sensors, attached by Velcro straps around their shanks and taped to each foot, all in the sagittal plane (Fig. 1). The center of the shank sensors were positioned two thirds of the distance to the knee from the ankle in order for the IMU's to sit flat against the shank. The superior edge of the foot sensors were placed to align with the lateral epicondyle of the ankle. A trial at each of the five speeds was recorded with subjects performing normal walking with their feet pointing forward. In the following five trials, subjects were instructed to partially turn their feet laterally, creating a toe-out walking condition.

D. Data Analysis

For each treadmill walking trial, only data recorded by sensors mounted on the right leg was used to estimate walking speeds. The mean walking speed was calculated by averaging the stride-by-stride data over the middle 40s data. Estimation error at a given speed was calculated as the difference between the estimated speed and the actual treadmill value. Within each condition, we averaged across subjects to determine the mean estimated speed (mean) and standard deviation (S.D.). The root mean square error (RMSE) of the speed estimates was calculated as

$$RMSE = \sqrt{\sum(estimated - actual)^2 / N} \qquad (7)$$

where N is the number of samples. The effects of sensor location (foot or shank) on the speed estimation error were then tested using one-way repeated-measures ANOVA for both the normal and toe-out walking conditions, with P< 0.05 considered statistically significant.

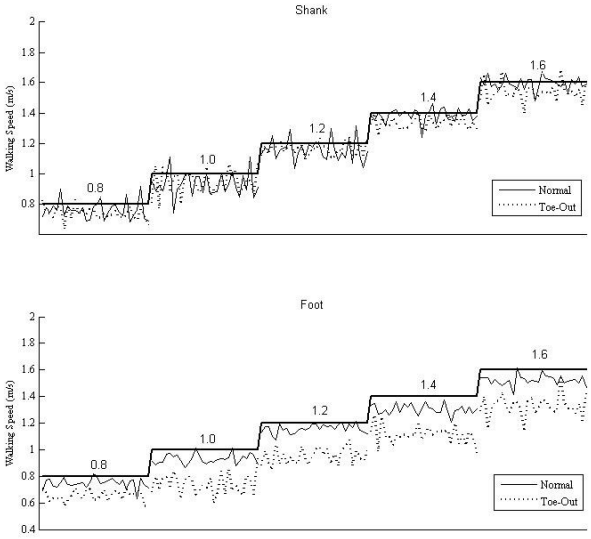

Figure 3 estimated walking speed from both shank- and foot-mounted sensors during normal and toe-out conditions from a representative subject during treadmill walking at speeds ranging from 0.8 to 1.6m/s

III. RESULTS

Using the directed walking speed estimation algorithms for both the shank- and foot-mounted IMU, the treadmill walking speeds were slightly underestimated in all cases. In comparison, the shank-mounted sensor achieved a better performance under both the normal and toe-out walking conditions than the foot-mounted sensor (Table 1). Fig. 3 presents typical data from a single subject during level walking. Comparing normal and toe-out conditions, it is observed that with the shank-mounted sensor, the estimated speeds were not affected under most of tested speeds (except the walking speed at 0.8m/s) under toe-out condition, yet results from the foot-mounted sensor showed a significant degradation at all walking speeds. These results are as expected because the change in sensor angle detected by the foot-mounted sensor in toe-out walking condition cannot be accounted for with the two degree of freedom acceleration measurements, resulting in lower velocity estimates. Fig. 4 presents mean± S.D. from all subjects walking at a treadmill speed of 1.2 m/s, generally considered as a comfortable walking speed. A statistical ANOVA analysis of estimated speeds calculated for the treadmill walking speed of 1.2 m/s yielded p-values of P=0.17 for the shank-mounted IMU estimations and P= 1.02e-04 for the foot-mounted IMU estimations.

Table 1 Walking speed estimation RMSE's at different treadmill speeds and walking conditions

Walking Conditions	Sensor Mounting Location	Speed (m/s)				
		0.8	1.0	1.2	1.4	1.6
Normal	Shank	0.02	0.09	0.06	0.09	0.07
	Foot	0.06	0.12	0.09	0.14	0.10
Toe-Out	Shank	0.06	0.09	0.10	0.08	0.09
	Foot	0.19	0.21	0.23	0.26	0.26

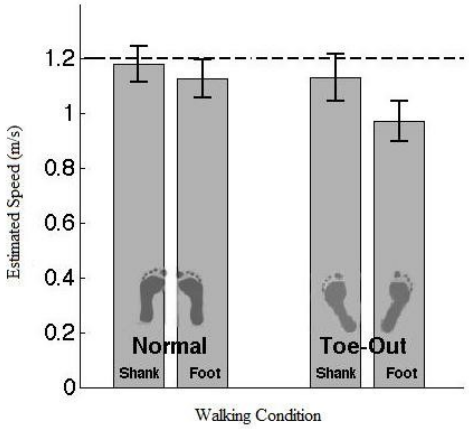

Figure 4 Mean estimated speeds from all 10 subjects during treadmill walking at a speed of 1.2 m/s during normal and toe-out.

IV. DISCUSSION

To date, numerous studies have been conducted estimating walking speeds from data collected through shank- and foot-mounted sensors [5-7,9-10]. The concurrent testing performed in this study allows for a direct comparison between algorithms from simultaneously collected shank- and foot-mounted sensor data during simple walking experiments. Through normal and toe-out walking conditions, algorithm performances in estimating walking speeds were compared to determine the preferred sensor location under different gait conditions.

While the algorithms compared proved accurate in estimating walking speeds for both shank and foot under normal walking conditions, this method, however, was not without error. This is partially due to the usage of only the accelerations in the sagittal plane instead of 3-axial acceleration and angular velocity measurements. This configuration results a simpler and cheaper walking speed estimation system. However, any deviation of the foot from the plane of progression causes the foot-mounted IMU sensor to measure accelerations in the third out-of sagittal plane axis. The sensor's local coordinate system therefore detects accelerations beyond the body's sagittal plane. Therefore, as sensor data is converted from the local to global coordinate system, a portion of the acceleration data is lost resulting in lower estimations of forward velocities. Deviation of the foot in toe-out walking condition also caused slight lateral deviations of the shank, resulting in a slight under-estimation of walking speed during toe-out walking as compared with the normal walking condition.

In summary, the speed estimation algorithm accuracy depends on the sensor location as well as the speed estimation algorithm. This study demonstrated that the distal located sensor will most likely be affected by the abnormal gait such as toe-out walking gait. Cautions need to be exercised when applying foot-mounted inertial sensor-based algorithm in estimating walking speeds for a pathological patient populations.

REFERENCES

[1] K. Tong and M. H. Granat. A practical gait analysis system using gyroscopes. *Med Eng Phys*, 21(2):87-94,1999

[2] A. T. Willemsen, J. A. van Alste, and H. B. Boom. Real-time gait assessment utilizing a new way of accelerometry. *Journal of Biomechanics*, 23(8):859-63, 1990

[3] J. M. Jasiewics, J. H. Allum, J. W. Middleton, A. Barriskill, P. Condie, B. Purcell, and R. C. Li. Gait event detection using linear accelerometers or angular velocity transducers in able-bodied and spinal-cord injured individuals. *Gait Posture*, 24(4):502-9, 2006.

[4] R. E. Mayagoitia, A. V. Nene, and P. H. Veltink. Accelerometer and rate gyroscope measurement of kinematics: an inexpensive alternative to optical motion analysis systems. *Journal of Biomechanics*, 35(4):537-42, 2002

[5] A. M. Sabatini, C. Martelloni, S. Scapellato, and F. Cavallo. Assessment of walking features from foot inertial sensing, *IEEE Transactions on Biomedical Engineering*, 52(3):486-94, 2005

[6] Q. Li, M. Young, V. Naing, and J. M. Donelan, Walking speed using a shank-mounted inertial measurement unit, *Journal of Biomechanics,* 43: 1640-1642, 2010

[7] Zijlstra W, Hof A. Assessment of spatio-temporal gait parameters from trunk accelerations during human walking. Gait Posture. 18(2):1–10, 2003

[8] D. Roetenberg, H. Luinge, and P. Slycke,. Xsens MVN: Full 6DOF Human Motion Tracking Using Miniature Inertial Sensors. *Xsens Technologies B.V.*, 2009.

[9] K. Aminan, B. Najafi, C. Büla, P.-F. Leyvraz, Ph. Robert, Spatio-temporal parameters of gait measured by an ambulatory system using miniature gyroscopes, *Journal of Biomechanics*, 35: 689-699, 2002

[10] Ö. Bebek, M. A. Suster, S. Rajgopal, M. J. Fu, X. Huang, M. C. Çavuşoğlu, D. J. Young, M. Mehregany, A. J. van den Bogert, C. H. Mastrangelo. Personal navigation via high-resolution gait-corrected inertial measurement units, *IEEE Transactions on Instrumentation and Measurement*, 59(11):3018-3026, 2010